A&A 374, 1127–1134 (2001)
DOI: 10.1051/0004-6361:20010784

Astronomy & Astrophysics

Polarization of the hydrogen Hα line in solar flares

Contribution of the local polarized radiation field and effect of the spectral index of the proton energy distribution

E. Vogt[1⋆], S. Sahal-Bréchot[2], and V. Bommier[2]

[1] Osservatorio Astronomico di Capodimonte, Via Moiariello 16, 80131 Napoli, Italy
e-mail: vogt@na.astro.it
[2] Observatoire de Paris-Meudon, DAMAp, CNRS UMR 8588 (Département Atomes et Molécules en Astrophysique), 5 Place Jules Janssen, 92195 Meudon Cedex, France
e-mail: Sylvie.Sahal-Brechot@obspm.fr, V.Bommier@obspm.fr

Received 3 April 2001 / Accepted 1 June 2001

Abstract. Linear polarization of the hydrogen Hα line was observed during solar flares. The polarization vector is directed towards disk center and its degree is of the order of 5%. The best explanation for this polarization is anisotropic collisional excitation of the $n = 3$ level of hydrogen by vertical beams of protons with an energy greater than a few keV. However, previous calculations gave an expected polarization degree of 2.5% or less, a factor of two below the observations. In this paper, the theoretical model for the formation of the line polarization has been refined, including the effect of polarization in the local radiation field that is created by hydrogen proton anisotropic excitation. We have also increased the spectral index of the proton energy distribution from 4 to 5, giving more weight to the low energy protons which are the most efficient for impact polarization, without ionizing the atmosphere too much. It is found that the inclusion of the polarization of the local radiation field does not increase the Hα polarization very significantly; however, going from a spectral index of 4 to 5 results in an expected polarization degree of 4.5%, compatible with the observations.

Key words. Sun: flares – polarization – atomic processes – line: formation

1. Introduction

A number of observations of linear polarization in the Hα line of hydrogen during solar flares have been reported (Hénoux et al. 1990; Metcalf et al. 1992, 1994; Vogt & Hénoux 1999). In all these observations, which measure the polarization integrated over the Hα line profile, the linear polarization degree is of the order of 5% and the direction of this polarization is in most cases close to the flare-to-disk-center direction, which we refer to as *radial polarization*.

These characteristics suggested that anisotropic collisional excitation of the hydrogen atoms by vertical beams of non-thermal protons may be the cause of the linear polarization observed. Protons accelerated at the magnetic reconnection site in the corona to energies greater than a few hundreds keV are able to reach the Hα line core formation level in the chromosphere without losing their directivity and with residual energies of a few tens of keV, causing anisotropic excitation of the hydrogen atoms (impact polarization) that leads to a linear polarization directed along the direction of the beam (Vogt & Hénoux 1996). By projection on the solar disk, this vertical direction appears as radial, directed towards the center of the disk.

In a previous paper (Vogt et al. 1997) that we will further refer to as Paper I, we computed the expected linear polarization degree due to proton impact excitation for 3 different atmospheric models, by solving the statistical equilibrium equations for a 3 main levels ($n = 1$ to $n = 3$) hydrogen atom. For the VAL F model (Vernazza et al. 1981) – used to represent the active region before the flare – the expected polarization degree was about 2.3%, accounting for the enhanced local electronic densities and line radiation caused by the proton bombardment. Starting with the MAVN F1 model (Machado et al. 1980) – representing an ongoing flare – the polarization degree dropped below 1%. Compared to the observed polarization of about 5%, these results were still significantly too low. We attributed this discrepancy to the limitations of the computation itself: we only had crude proton-hydrogen cross-sections available at that time and we didn't take

Send offprint requests to: E. Vogt,
e-mail: etienne@astro.gla.ac.uk
⋆ *Present address:* Department of Physics and Astronomy, University of Glasgow, Glasgow G12 8QQ, UK.

into account the effect of the local radiation field polarization, polarization that is itself created by the proton impact excitation.

Later, new cross-sections for proton-hydrogen collisions, based on close-coupling calculations were made available (Balança & Feautrier 1998). New computations using these cross-sections and adding the charge exchange transitions, which also contribute to line center polarization through the double charge exchange process, were published in the *2nd Solar Polarization Workshop* proceedings (Vogt et al. 1999). These gave for the base model VAL F a maximum polarization degree of 2.5%, a little higher than before, but still significantly below the observations.

In this paper, we introduce the polarization of the local radiation field in the statistical equilibrium equations, using the optically thick limit solution for the radiative transfer equation. Starting from a non-polarized radiation field, we solve the statistical equilibrium equations iteratively, reintroducing the line radiation polarization found at the preceeding step. We also investigate the effect of varying the spectral index of the proton number flux energy distribution, a parameter which has been kept constant in the previous computations. Going to higher spectral indexes (from 4 to 5) will concentrate the energy distribution more towards low energies, which will reduce the ionization rates and thus the depolarising collisions due to background thermal electrons and protons. These two improvements should both contribute to raise the expected polarization degree.

2. Model parameters

2.1. Solar atmosphere

As in paper I, the solar atmosphere will be described by semi-empirical models. We will use the VAL F model as representing the atmosphere of an active region at the beginning of a flare and the MAVN F1 model as representing the heated atmosphere at the maximum of Hα emission. Both these models are modified to account for the effects of the proton beam bombardment on the local electron and proton densities and on the hydrogen line intensities. This is done by running a computer code developped by Fang & Hénoux (Fang et al. 1993) which solves non-polarized radiative transfer equations together with non-LTE statistical equilibrium equations including non-thermal proton collision rates, for a proton number flux $\mathcal{F}$ between 10^{14} and 10^{17} cm^{-2} s^{-1}, a power law proton number flux energy distribution of spectral index $\delta = 4$ or 5 and an initial low energy threshold at the injection site in the corona of 150 keV.

We will no longer use the VAL C model (average quiet Sun) as it is not really suitable for describing any stage of a flare. Also, we choose to ignore the MAVN F2 model, which describes a bright flare, but using only thermal processes, thus requiring very large local electron and proton densities at the Hα line core formation level, of the order of 10^{13} cm^{-3}. Such high densities would lead to complete depolarization of the line. Indeed, the fainter F1 model, with the added non-thermal effects gives hydrogen line emissions comparable to those of the hotter F2 model. Similarly, the VAL F model gives enhanced line emissions when the non-thermal effects are added.

2.2. Statistical equilibrium equations

As in Paper I, the statistical equilibrium equations are written on the basis of the irreducible tensorial operators. The same symmetry considerations allow us to consider only diagonal density matrix elements ${}^{nlj}\rho^k_q$ with $q = 0$ and k even. The equations are written for each level $n'l'j'$ and its corresponding multipolar orders $k' = 0, ..., 2j'$ as:

$$\sum_{nlj,k} \Pi_{nlj,k\rightarrow n'l'j',k'} {}^{nlj}\rho^k_0 = 0. \quad (1)$$

The statistical equilibrium coefficients $\Pi_{nlj,k\rightarrow n'l'j',k'}$ divide themselves into two groups. Those coupling two different nlj levels are the sum of a radiative rate $R_{k\rightarrow k',nlj\rightarrow n'l'j'}$ and a collisional rate $C_{k\rightarrow k',nlj\rightarrow n'l'j'}$:

$$\Pi_{nlj,k\rightarrow n'l'j',k'} = C_{k\rightarrow k',nlj\rightarrow n'l'j'} + R_{k\rightarrow k',nlj\rightarrow n'l'j'}, \quad (2)$$

whereas the others, representing the relaxation of a level nlj, are expressed as a negative sum of radiative relaxation rates $R^{\rm relax}_{k\rightarrow k',nlj\rightarrow n'l'j'}$ and collisional relaxation rates $C^{\rm relax}_{k\rightarrow k',nlj\rightarrow n'l'j'}$ over all the possible relaxation paths $nlj \rightarrow n'l'j'$:

$$\begin{aligned}\Pi_{nlj,k\rightarrow nlj,k'} \;=\; & -\sum_{n'l'j'\neq nlj} C^{\rm relax}_{k\rightarrow k',nlj\rightarrow n'l'j'} \\ & -\sum_{n'l'j'\neq nlj} R^{\rm relax}_{k\rightarrow k',nlj\rightarrow n'l'j'}. \end{aligned} \quad (3)$$

2.3. Collisional rates

The depolarizing collisions with the thermal background electrons and protons will be treated as in Paper I, using the semi-classical perturbation approximation (Sahal-Bréchot et al. 1996).

For the polarizing non-thermal collisions with the protons of the beam, we will use the close-coupling proton hydrogen cross-sections from Balança (1997) and Balança et al. (1998). As these authors give the excitation and charge exchange cross sections $\sigma^{0\rightarrow k'}_{1s\rightarrow n'l'}$ from fundamental level 1s to excited levels $n'l'$ and multipolar order k' without taking into account fine structure splitting, we have first to obtain from these the cross sections for excitation and charge exchange $\sigma^{0\rightarrow k'}_{1s\frac{1}{2}\rightarrow n'l'j'}$ towards fine structure levels $n'l'j'$. As the collision energies are large compared to the fine structure separation of the levels, the relation between the two cross sections just involves some angular algebra coefficients and is given by Feautrier (1999):

$$\begin{aligned}\sigma^{0\rightarrow k'}_{1s\frac{1}{2}\rightarrow n'l'j'} \;=\; & \frac{1}{\sqrt{2}}(2j'+1)(-1)^{-j'-l'-k'-\frac{1}{2}} \left\{ \begin{array}{ccc} l' & l' & k' \\ j' & j' & \frac{1}{2} \end{array} \right\} \\ & \times\sigma^{0\rightarrow k'}_{1s\rightarrow n'l'}, \end{aligned} \quad (4)$$

where the entity in chain brackets is a so-called *6j* coefficient. We then obtain the collisional transition rates $C_{0\rightarrow k',1s\frac{1}{2}\rightarrow n'l'j'}$ by integrating the cross sections over the velocity distribution of the proton beam as:

$$C_{0\rightarrow k',1s\frac{1}{2}\rightarrow n'l'j'} = N_{\rm P}\int_{v_0}^{\infty}\sigma_{1s\frac{1}{2}\rightarrow n'l'j'}^{0\rightarrow k'}(v_z)f(v_z){\rm d}v_z, \quad (5)$$

where $f(v_z)$ is the velocity distribution function corresponding to a vertical beam with a power law energy distribution of spectral index δ, given by:

$$f(v_z){\rm d}v_z = \frac{2\delta-2}{v_0}\left(\frac{v_z}{v_0}\right)^{1-2\delta}{\rm d}v_z, \;\; v_z \geq v_0, \quad (6)$$

$N_{\rm P}$ is the non-thermal proton density at the Hα line core formation level (Vogt 1997):

$$N_{\rm P} = \frac{2\delta-3}{2\delta-2}\times\frac{\mathcal{F}}{v_0} \quad (7)$$

and $v_0 = \sqrt{\frac{2E_0}{m_{\rm P}}}$ is the velocity threshold corresponding to the lower energy threshold E_0 of the proton energy distribution at the line formation level (from 1 to 20 keV).

Finally, since there are no proton-hydrogen close-coupling cross sections available for transitions from $n = 2$ to $n = 3$, we will neglect these transitions and consider only the non-thermal transitions from the fundamental level. Since the relative populations of the higher levels are very low (less than 10^{-6} in all cases), the non-thermal transitions from these higher levels should not play any significant role in the statistical equilibrium equations.

2.4. Radiative rates

In Paper I, we wrote the radiative transition and relaxation rates $R_{k\rightarrow k',nlj\rightarrow n'l'j'}$ and $R^{\rm relax}_{k\rightarrow k',nlj\rightarrow n'l'j'}$ respectively as:

$$\begin{aligned} R_{k\rightarrow k',nlj\rightarrow n'l'j'} &= \delta_{k,k'}c^{(0)}_{k,j\rightarrow j'}\gamma^{(0)}_{nlj\rightarrow n'l'j'} \\ &\quad + c^{(2)}_{k\rightarrow k',j\rightarrow j'}\gamma^{(2)}_{nlj\rightarrow n'l'j'} \quad (8) \\ R^{\rm relax}_{k\rightarrow k',nlj\rightarrow n'l'j'} &= \delta_{k,k'}c^{{\rm relax}\ (0)}_{k,j\rightarrow j'}\gamma^{(0)}_{nlj\rightarrow n'l'j'} \\ &\quad + c^{{\rm relax}\ (2)}_{k\rightarrow k',j\rightarrow j'}\gamma^{(2)}_{nlj\rightarrow n'l'j'}, \quad (9) \end{aligned}$$

where $\delta_{k,k'}$ is a Kronecker symbol, $\gamma^{(0)}_{nlj\rightarrow n'l'j'}$ and $\gamma^{(2)}_{nlj\rightarrow n'l'j'}$ are the radiative contributions respectively to population and alignment, and $c^{(0)}_{k,j\rightarrow j'}$, $c^{(2)}_{k\rightarrow k',j\rightarrow j'}$, $c^{{\rm relax}\ (0)}_{k,j\rightarrow j'}$ and $c^{{\rm relax}\ (2)}_{k\rightarrow k',j\rightarrow j'}$ are angular algebra coefficients defined in Sahal-Bréchot et al. (1996) as:

$$\begin{aligned} c^{(0)}_{k,j\rightarrow j'} &= (-1)^{j+j'+k+1}(2j+1)\left\{\begin{array}{ccc} j & j & k \\ j' & j' & 1\end{array}\right\} \quad (10) \\ c^{(2)}_{k\rightarrow k',j\rightarrow j'} &= (-1)^k(2j+1)\sqrt{\frac{15}{2}(2k+1)(2k'+1)} \\ &\quad \times\left(\begin{array}{ccc} k & k' & 2 \\ 0 & 0 & 0\end{array}\right)\left\{\begin{array}{ccc} j & j & k \\ j' & j' & k' \\ 1 & 1 & 2\end{array}\right\} \quad (11) \end{aligned}$$

$$\begin{aligned} c^{{\rm relax}\ (0)}_{k,j\rightarrow j'} &= 1 \quad (12) \\ c^{{\rm relax}\ (2)}_{k\rightarrow k',j\rightarrow j'} &= (-1)^{j-j'+1}(2j+1)\sqrt{\frac{15}{2}(2k+1)(2k'+1)} \\ &\quad \times\left(\begin{array}{ccc} k & k' & 2 \\ 0 & 0 & 0\end{array}\right)\left\{\begin{array}{ccc} k & k' & 2 \\ j & j & j\end{array}\right\}\left\{\begin{array}{ccc} 1 & 1 & 2 \\ j & j & j'\end{array}\right\}. \quad (13) \end{aligned}$$

At that time, we neglected the alignment contribution term since we supposed that the local radiation field was both isotropic and unpolarized. In fact, a significant part of this local radiation field comes from photons emitted by atoms that have been excited by the proton beam and these photons are linearly polarized. This should be taken into account in the statistical equilibrium equations as these photons can transfer their polarization to other atoms when absorbed. A full treatment would require solving together the polarized radiative transfer equations and the statistical equilibrium equations, which is a quite complicated task. However, in the optically thick limit, which holds for Lyα and Lyβ at the Hα line core formation level (Hα itself is not really optically thick here, but we will treat it in the same way, as its contribution to populating the $n = 3$ level is significantly less than the Lyβ one), we can use the asymptotic solution of the radiative transfer equation to get an analytic expression for the radiative contribution terms in function of the polarization of the emitted radiation and solve the statistical equilibrium equations iteratively, starting from zero initial polarization (there is no significant polarization before the flare) and iterating, reintroducing the polarization found previously, until it converges.

Landi Degl'Innocenti (1984) gives the following expressions for the radiative transition and relaxation rates that involve absorption of radiation (Eqs. (51) and (54) of his paper). As in Paper I, symmetry considerations allow us to discard all terms with $q \neq 0$ and to keep only the $k = 0$ (population) and $k = 2$ (alignment) terms. Also, we can neglect the anomalous dispersion terms for hydrogen lines in the solar chromosphere. Transcribing his notations into ours, we have the following expressions for the radiative rates:

$$\begin{aligned} R_{k\rightarrow k',nlj\rightarrow n'l'j'} &= \sum_{K=0,2}(2j+1) \\ &\quad \times\sqrt{3(2k'+1)(2k+1)(2K+1)} \\ &\quad \times\left\{\begin{array}{ccc} 1 & j' & j \\ 1 & j' & j \\ K & k' & k\end{array}\right\}\left(\begin{array}{ccc} k' & k & K \\ 0 & 0 & 0\end{array}\right) \\ &\quad \times B_{nlj\rightarrow n'l'j'}\bar{J}^K_0(\nu_{n'\rightarrow n}) \quad (14) \\ R^{\rm relax}_{k\rightarrow k',nlj\rightarrow n'l'j'} &= \sum_{K=0,2}(2j+1)(-1)^{1+j-j'} \\ &\quad \times\sqrt{3(2k'+1)(2k+1)(2K+1)} \\ &\quad \times\left\{\begin{array}{ccc} 1 & 1 & K \\ j & j & j'\end{array}\right\}\left\{\begin{array}{ccc} k & k' & K \\ j & j & j\end{array}\right\}\left(\begin{array}{ccc} k & k' & K \\ 0 & 0 & 0\end{array}\right) \\ &\quad \times B_{nlj\rightarrow n'l'j'}\bar{J}^K_0(\nu_{n'\rightarrow n}), \quad (15) \end{aligned}$$

where $B_{nlj\rightarrow n'l'j'}$ is the Einstein coefficient for absorption of radiation in the transition considered and $\bar{J}^K_0(\nu_{n'\rightarrow n})$ is the K order component of the radiation field tensor integrated over the line absorption profile. $\bar{J}^0_0$ is just the profile integrated mean intensity (that we called I_ν in Paper I, even if it is not a specific intensity), and $\bar{J}^2_0$ is the alignment component that we want to introduce. Comparing these expressions with the previous Eqs. (8) and (9) and using the usual symmetry relations for *3j*, *6j* and *9j* coefficients, we find the following expressions for the radiative absorption contributions:

$$\gamma^{(0)}_{nlj\rightarrow n'l'j'} = B_{nlj\rightarrow n'l'j'}\bar{J}^0_0(\nu_{n'\rightarrow n}) \quad (16)$$

$$\gamma^{(2)}_{nlj\rightarrow n'l'j'} = \sqrt{2}\, B_{nlj\rightarrow n'l'j'}\bar{J}^2_0(\nu_{n'\rightarrow n}). \quad (17)$$

As, for the radiative emission terms, they are the same as in Paper I:

$$\gamma^{(0)}_{n'l'j'\rightarrow nlj} = A_{n'l'j'\rightarrow nlj} \quad (18)$$

$$\gamma^{(2)}_{n'l'j'\rightarrow nlj} = 0. \quad (19)$$

Induced emission has been neglected, as it is much smaller than spontaneous emission for chromospheric hydrogen lines. Also, the latter being an isotropic process, there is no alignment term associated with it.

So, we now need to find an expression for $\bar{J}^2_0$ as a function of the polarization of the radiation emitted by the other local atoms. $\bar{J}^K_Q$ is defined as (Landi Degl'Innocenti 1984):

$$\bar{J}^K_Q = \oint \frac{\mathrm{d}\Omega}{4\pi}\sum_{i=0}^{3}\mathcal{T}^K_Q(i,\Omega)\bar{\mathcal{I}}_i(\Omega), \quad (20)$$

where the $\bar{\mathcal{I}}_i(\Omega) = \bar{I},\bar{Q},\bar{U},\bar{V}$ $(i = 0{-}3)$ are the profile averaged Stokes parameters of the incident radiation in direction Ω (we use line profile averaged quantities here as we are only interested in profile averaged polarization) and the $\mathcal{T}^K_Q(i,\Omega)$ are the irreducible spherical tensors for polarimetry defined in Appendix 1 of Landi Degl'Innocenti (1984).

Normally, the $\bar{\mathcal{I}}_i(\Omega)$ should be obtained by solving the polarized radiative transfer equations. However, for the optically thick (at Hα formation level) Lyα and Lyβ lines, we can use the asymptotic limit for great optical depths: $\bar{\mathcal{I}}_i(\Omega) \approx \bar{\mathcal{S}}_i(\Omega)$, the source function for the i Stokes parameter. If we further assume that the absorption matrix is diagonal – neglecting any process that could affect the polarization of the radiation between its emission and its absorption, like the Hanle effect – and reduces to a scalar absorption coefficient κ_I, we can write:

$$\bar{\mathcal{I}}_i(\Omega) \approx \frac{\bar{\mathcal{E}}_i(\Omega)}{\kappa_\mathrm{I}}, \quad (21)$$

introducing the emissivity in Stokes parameter i, $\bar{\mathcal{E}}_i(\Omega)$, giving the following approximation for the radiation tensor:

$$\bar{J}^K_Q \approx \frac{1}{\kappa_I}\oint \frac{\mathrm{d}\Omega}{4\pi}\sum_{i=0}^{3}\mathcal{T}^K_Q(i,\Omega)\bar{\mathcal{E}}_i(\Omega). \quad (22)$$

Still following Landi Degl'Innocenti (1984), the emissivity can be written as:

$$\bar{\mathcal{E}}_i(\Omega,\nu_{n'\rightarrow n}) = \frac{h\nu_{n'\rightarrow n}}{4\pi}N_\mathrm{H}\sum_{l'j'\rightarrow lj}A_{n'l'j'\rightarrow nlj}\sqrt{2j'+1} \times\sum_{K',Q'}w^{(K')}_{j'\rightarrow j}\mathcal{T}^{K'}_{Q'}(i,\Omega)\,{}^{n'l'j'}\rho^{K'}_{Q'}, \quad (23)$$

where $A_{n'l'j'\rightarrow nlj}$ is the Einstein coefficient for spontaneous emission, N_H is the local hydrogen density, $w^{(K')}_{j'\rightarrow j}$ is the ratio of 2 *6j* coefficients defined in Landi Degl'Innocenti (1984) Eq. (38) and ${}^{n'l'j'}\rho^{K'}_{Q'}$ is a density matrix element as they appear in the statistical equilibrium equations. Again, induced emission has been neglected as well as the so-called "Rayleigh diffusion term" (Bommier 1997) which is only of interest when partial frequency redistribution effects are considered. We now replace this expression in Eq. (22), to get:

$$\bar{J}^K_Q(\nu_{n'\rightarrow n}) \approx \frac{h\nu_{n'\rightarrow n}}{4\pi\kappa_I(\nu_{n'\rightarrow n})}N_\mathrm{H}\sum_{l'j'\rightarrow lj}A_{n'l'j'\rightarrow nlj}\sqrt{2j'+1} \times\sum_{K',Q'}w^{(K')}_{j'\rightarrow j}\mathcal{A}^{K,K'}_{Q,Q'}\,{}^{n'l'j'}\rho^{K'}_{Q'}, \quad (24)$$

with

$$\mathcal{A}^{K,K'}_{Q,Q'} = \sum_{i=0}^{3}\oint\frac{\mathrm{d}\Omega}{4\pi}\mathcal{T}^K_Q(i,\Omega)\mathcal{T}^{K'}_{Q'}(i,\Omega). \quad (25)$$

This integral can be calculated using the definitions of the $\mathcal{T}^K_Q$ in Landi Degl'Innocenti (1984), giving the following expression:

$$\mathcal{A}^{K,K'}_{Q,Q'} = \mathcal{A}^{(K)}\,\delta_{K,K'}\,\delta_{Q,-Q'}, \quad (26)$$

with $\mathcal{A}^{(0)} = 1$ for mean intensity, $\mathcal{A}^{(1)} = \frac{1}{2}$ for orientation and $\mathcal{A}^{(2)} = \frac{7}{10}$ for alignment. So we arrive at the following final expression for the radiation tensor:

$$\bar{J}^K_Q(\nu_{n'\rightarrow n}) \approx \frac{h\nu_{n'\rightarrow n}}{4\pi\kappa_I(\nu_{n'\rightarrow n})}N_\mathrm{H}\mathcal{A}^{(K)}\sum_{l'j'\rightarrow lj}A_{n'l'j'\rightarrow nlj} \times\sqrt{2j'+1}\,w^{(K)}_{j'\rightarrow j}\,{}^{n'l'j'}\rho^K_{-Q}. \quad (27)$$

In particular, the ratio of the radiation alignment over the mean intensity can be expressed as:

$$\frac{\bar{J}^2_0(\nu_{n'\rightarrow n})}{\bar{J}^0_0(\nu_{n'\rightarrow n})} = \frac{\mathcal{A}^{(2)}}{\mathcal{A}^{(0)}} \times\frac{\sum_{l'j'\rightarrow lj}A_{n'l'j'\rightarrow nlj}\sqrt{2j'+1}\,w^{(2)}_{j'\rightarrow j}\,{}^{n'l'j'}\rho^2_0}{\sum_{l'j'\rightarrow lj}A_{n'l'j'\rightarrow nlj}\sqrt{2j'+1}\,w^{(0)}_{j'\rightarrow j}\,{}^{n'l'j'}\rho^0_0} = \frac{7}{10}\,2\sqrt{2}\,\eta_{n'\rightarrow n}, \quad (28)$$

using the $\eta_{n'\rightarrow n}$ quantity defined in Paper I, Eq. (27). With the mean intensity given by the non-polarized radiative transfer code, we can finally express the alignment

radiative contribution $\gamma^{(2)}$ as a function of the mean intensity and the η polarization factor as:

$$\gamma^{(2)}_{nlj\to n'l'j'} = 4\,\frac{7}{10}\,\eta_{n'\to n} B_{nlj\to n'l'j'}\,\bar{J}^0_0(\nu_{n'\to n}). \quad (29)$$

This expression can be used in a straightforward way to introduce the alignment contribution of the local radiation field in the statistical equilibrium equations, using the η factors that were obtained on the previous iteration.

2.5. Polarization degree

The maximum linear polarization degree (observed at a 90 degrees angle from the beam), is obtained from the η factor by the following expression:

$$\tau_{90,n'\to n} = -\frac{3\eta_{n'\to n}}{1-\eta_{n'\to n}}. \quad (30)$$

This is similar to Eq. (28) in Paper I except for the minus sign, which comes from a different sign convention used in the definition of the Stokes Q emissivity (Eq. (23) of this paper versus Eq. (24) of Paper I). The previous sign convention gives in fact a negative polarization degree (proton excitation at the energies considered creates negative alignment) which was not coherent with the results shown in the same paper or the observation papers (Vogt & Hénoux 1996, 1999).

3. Results and discussion

The Hα maximum linear polarization degree τ_{90} has been computed for the base models VAL F and MAVN F1, with a proton spectral index δ of either 4 or 5. The lower energy threshold E_0 of the proton energy distribution at Hα formation level in the chromosphere has been varied between 1 and 20 keV and the proton number flux $\mathcal{F}$ between 1×10^{14} and 2×10^{17} cm^{-2} s^{-1} for the VAL F model and between 1×10^{16} and 1×10^{19} cm^{-2} s^{-1} for the F1 model. The results are shown in Tables 1 to 4. All these calculations include the effect of the polarization in the local radiation field.

If we compare the results obtained for the VAL F model and $\delta = 4$ (Table 1) to the ones obtained previously without the effect of the background radiation polarization (Balança & Vogt 1999) (Balança & Vogt 2001) (Vogt et al. 1999), we see that, contrary to our initial expectations, the effect of this polarization in the local radiation is rather small, reinforcing the polarization only by a small fraction. The maximum polarization predicted in this case is now 2.6%, compared to 2.5% previously, and so is still significantly lower than the typical observed polarization degree of 3–6%. Similarly, in the case of the MAVN F1 model (Table 3), the maximum polarization expected is of the order of 0.7%, comparable to the values obtained in Paper I. However, we should note that the iterative process of reintroducing the emitted radiation polarization into the statistical equilibrium equations converges very well, reaching a less than 10^{-5} relative correction on the Hα polarization degree in less than 10 iterations. We have also verified that the same final result is obtained if we start from a fully polarized local radiation field instead of an unpolarized one. So it is clear that this smaller than expected correction is not due to numerical computation problems, but that taking into account the linear polarization of the radiation field at the origin of the radiative excitation is not enough to significantly boost the Hα line polarization degree.

On the other hand, using a spectral index of 5 gives a very significant increase in the polarization degree, with a maximum value of 4.7% for the VAL F atmosphere (Table 2). This appears clearly in Fig. 1, where the polarization degree for $\delta = 5$ (plain line) and $\delta = 4$ (dotted line) are plotted together as a function of the proton number flux $\mathcal{F}$, the lower energy threshold E_0 being set to the value leading to maximal polarization (4 keV for $\delta = 5$ and 7 keV for $\delta = 4$). We can see on this graph that the polarization degrees for the two values of δ are similar up to a flux of a few 10^{15} cm^{-2} s^{-1}, after which the curve for $\delta = 4$ starts to curve downward, peaking at 2.6% for a flux of 10^{16} cm^{-2} s^{-1}, whereas the curve for $\delta = 5$ continues to rise and finally peaks at 4.8% when the flux reaches 5×10^{16} cm^{-2} s^{-1}. This difference is due to the highest proportion of high energy protons in the $\delta = 4$ proton energy distribution. These high energy protons (100 keV and above) cause ionization of the ambient hydrogen atoms and raise the local electron and protons densities, thus producing larger depolarizing collisional rates. It is this rise of the depolarizing collisions that finally causes the polarization to decrease at high fluxes. If these depolarizing rates are reduced because of a proton energy distribution more concentrated towards low energies, the polarization can reach higher values. A similar increase of the maximum polarization is obtained with the hot F1 model, where the polarization can reach 1.2% with a $\delta = 5$ distribution instead of 0.7% for $\delta = 4$ (Table 4 and Fig. 2).

In Figs. 3 and 4, we have also represented the Hα polarization degree as a function of the proton lower energy threshold at chromospheric level. For $\delta = 4$, the curves are rather flat between 4 and 15 keV, whereas for $\delta = 5$, they are more clearly peaked around 4–5 keV. This is due to the fact that an energy distribution more peaked towards low energies will cause less smoothing of the excitation cross sections when the integration in Eq. (5) is performed. In any case, the precise value of this lower energy threshold is not critical for the polarization degree and will indeed no longer be a free parameter when a more sophisticated model fully including energy deposit into the atmosphere by the proton beam and the resulting evolution of the beam energy distribution function will be available.

The results obtained here are much more compatible with the observed Hα polarization degrees of 3–6%, (Vogt & Hénoux 1999) than those in Paper I, which implies that the non-thermal protons at the origin of the observed polarization must have a rather soft energy distribution with

Table 1. Hα polarization degree τ_{90} for the initial atmospheric model VAL F and proton spectral index $\delta = 4$ as a function of chromospheric level lower energy threshold E_0 (in keV) and proton number flux $\mathcal{F}$ (in particles $\mathrm{cm}^{-2}\,\mathrm{s}^{-1}$).

$\mathcal{F} \setminus E_0$	1 keV	2 keV	3 keV	4 keV	5 keV	7 keV	10 keV	15 keV	20 keV
1×10^{14}	0.02%	0.05%	0.07%	0.09%	0.10%	0.12%	0.13%	0.14%	0.12%
2×10^{14}	0.04%	0.09%	0.14%	0.18%	0.20%	0.23%	0.26%	0.27%	0.23%
5×10^{14}	0.09%	0.22%	0.33%	0.42%	0.47%	0.53%	0.58%	0.60%	0.52%
1×10^{15}	0.17%	0.40%	0.61%	0.75%	0.84%	0.94%	1.02%	1.04%	0.89%
2×10^{15}	0.30%	0.68%	1.02%	1.25%	1.37%	1.49%	1.59%	1.60%	1.37%
5×10^{15}	0.54%	1.17%	1.68%	1.99%	2.13%	2.24%	2.30%	2.26%	1.93%
1×10^{16}	0.70%	1.47%	2.05%	2.36%	2.48%	2.55%	2.54%	2.45%	2.09%
2×10^{16}	0.75%	1.52%	2.08%	2.35%	2.43%	2.45%	2.41%	2.31%	1.96%
5×10^{16}	0.71%	1.39%	1.86%	2.07%	2.10%	2.09%	2.02%	1.92%	1.63%
1×10^{17}	0.64%	1.23%	1.63%	1.78%	1.80%	1.77%	1.70%	1.60%	1.36%

Table 2. Hα polarization degree τ_{90} for the initial atmospheric model VAL F and proton spectral index $\delta = 5$ as a function of chromospheric level lower energy threshold E_0 (in keV) and proton number flux $\mathcal{F}$ (in particles $\mathrm{cm}^{-2}\,\mathrm{s}^{-1}$).

$\mathcal{F} \setminus E_0$	1 keV	2 keV	3 keV	4 keV	5 keV	7 keV	10 keV	15 keV	20 keV
1×10^{14}	0.02%	0.04%	0.07%	0.09%	0.10%	0.11%	0.13%	0.15%	0.13%
2×10^{14}	0.03%	0.08%	0.13%	0.17%	0.19%	0.22%	0.26%	0.28%	0.25%
5×10^{14}	0.08%	0.19%	0.32%	0.41%	0.47%	0.54%	0.61%	0.67%	0.58%
1×10^{15}	0.15%	0.37%	0.61%	0.78%	0.88%	0.99%	1.11%	1.19%	1.03%
2×10^{15}	0.29%	0.69%	1.11%	1.40%	1.56%	1.71%	1.86%	1.95%	1.69%
5×10^{15}	0.64%	1.43%	2.20%	2.65%	2.86%	2.99%	3.10%	3.12%	2.68%
1×10^{16}	1.05%	2.20%	3.21%	3.69%	3.87%	3.90%	3.87%	3.79%	3.25%
2×10^{16}	1.55%	2.95%	4.07%	4.50%	4.58%	4.47%	4.29%	4.11%	3.51%
5×10^{16}	2.04%	3.47%	4.50%	4.74%	4.70%	4.44%	4.15%	3.91%	3.33%
1×10^{17}	2.13%	3.39%	4.27%	4.39%	4.30%	4.00%	3.69%	3.46%	2.94%
2×10^{17}	2.03%	3.04%	3.75%	3.81%	3.69%	3.40%	3.12%	2.91%	2.48%

Table 3. Hα polarization degree τ_{90} for the initial atmospheric model MAVN F1 and proton spectral index $\delta = 4$ as a function of chromospheric level lower energy threshold E_0 (in keV) and proton number flux $\mathcal{F}$ (in particles $\mathrm{cm}^{-2}\,\mathrm{s}^{-1}$).

$\mathcal{F} \setminus E_0$	1 keV	2 keV	3 keV	4 keV	5 keV	7 keV	10 keV	15 keV	20 keV
1×10^{16}	0.003%	0.008%	0.01%	0.02%	0.02%	0.02%	0.02%	0.02%	0.02%
2×10^{16}	0.006%	0.02%	0.02%	0.03%	0.03%	0.04%	0.04%	0.05%	0.04%
5×10^{16}	0.02%	0.04%	0.06%	0.07%	0.08%	0.09%	0.10%	0.11%	0.09%
1×10^{17}	0.03%	0.07%	0.10%	0.13%	0.14%	0.16%	0.18%	0.19%	0.16%
2×10^{17}	0.05%	0.12%	0.18%	0.23%	0.25%	0.28%	0.30%	0.31%	0.26%
5×10^{17}	0.10%	0.23%	0.33%	0.40%	0.43%	0.46%	0.48%	0.47%	0.40%
1×10^{18}	0.15%	0.33%	0.47%	0.54%	0.57%	0.59%	0.59%	0.57%	0.49%
2×10^{18}	0.20%	0.41%	0.55%	0.62%	0.64%	0.64%	0.63%	0.61%	0.51%
5×10^{18}	0.25%	0.48%	0.63%	0.68%	0.68%	0.67%	0.64%	0.60%	0.51%
1×10^{19}	0.25%	0.46%	0.59%	0.64%	0.64%	0.63%	0.60%	0.56%	0.48%

a spectral index around 5 below 1 MeV and a particle number flux of a few 10^{16} $\mathrm{cm}^{-2}\,\mathrm{s}^{-1}$. This can be used to constrain proton acceleration models. It should be noted that since our modified atmospheric models do not yet take into account the energy balance, particle fluxes in excess of 5×10^{16} $\mathrm{cm}^{-2}\,\mathrm{s}^{-1}$ are no longer compatible with the thermal structure of the VAL F model (more energy is deposited by the proton beam than can be radiated away, even when considering the enhanced line emission that the proton bombardment produces). It is thus more reasonable to use the hotter MAVN F1 model for proton fluxes between 10^{17} and 5×10^{18} $\mathrm{cm}^{-2}\,\mathrm{s}^{-1}$ (limit at which

Table 4. Hα polarization degree τ_{90} for the initial atmospheric model MAVN F1 and proton spectral index $\delta = 5$ as a function of chromospheric level lower energy threshold E_0 (in keV) and proton number flux $\mathcal{F}$ (in particles $\mathrm{cm}^{-2}\,\mathrm{s}^{-1}$).

$\mathcal{F} \setminus E_0$	1 keV	2 keV	3 keV	4 keV	5 keV	7 keV	10 keV	15 keV	20 keV
1×10^{16}	0.003%	0.006%	0.01%	0.01%	0.02%	0.02%	0.02%	0.03%	0.02%
2×10^{16}	0.005%	0.01%	0.02%	0.03%	0.03%	0.04%	0.04%	0.05%	0.04%
5×10^{16}	0.01%	0.03%	0.05%	0.07%	0.08%	0.09%	0.10%	0.11%	0.10%
1×10^{17}	0.02%	0.06%	0.10%	0.12%	0.14%	0.16%	0.19%	0.20%	0.18%
2×10^{17}	0.05%	0.11%	0.19%	0.24%	0.27%	0.30%	0.33%	0.36%	0.31%
5×10^{17}	0.11%	0.26%	0.41%	0.50%	0.54%	0.58%	0.61%	0.63%	0.54%
1×10^{18}	0.19%	0.42%	0.63%	0.74%	0.78%	0.80%	0.80%	0.80%	0.68%
2×10^{18}	0.31%	0.62%	0.88%	0.98%	1.00%	0.98%	0.95%	0.92%	0.78%
5×10^{18}	0.49%	0.84%	1.10%	1.16%	1.15%	1.07%	1.00%	0.95%	0.81%
1×10^{19}	0.57%	0.90%	1.13%	1.15%	1.12%	1.04%	0.95%	0.90%	0.76%
2×10^{19}	0.61%	0.90%	1.10%	1.11%	1.07%	0.97%	0.89%	0.83%	0.70%

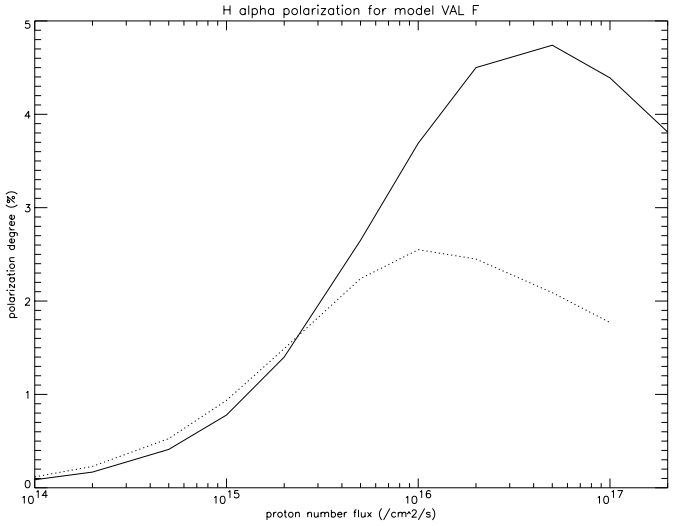

Fig. 1. Hα polarization degree (in percent) as a function of the proton number flux (in particles $\mathrm{cm}^{-2}\,\mathrm{s}^{-1}$) for the initial atmospheric model VAL F, for $\delta = 5$, $E_0 = 4$ keV (plain line) and $\delta = 4$, $E_0 = 7$ keV (dotted line).

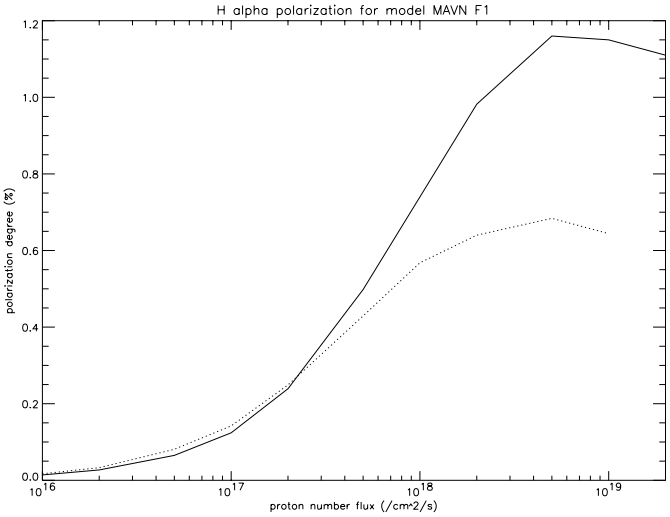

Fig. 2. Hα polarization degree (in percent) as a function of the proton number flux (in particles $\mathrm{cm}^{-2}\,\mathrm{s}^{-1}$) for the initial atmospheric model MAVN F1, for $\delta = 5$, $E_0 = 4$ keV (plain line) and $\delta = 4$, $E_0 = 5$ keV (dotted line).

the F1 thermal structure breaks down as well). Since this model predicts much lower polarization, it can be expected that the polarization signal will be much lower during the hottest phase of a flare. Such an effect was indeed seen for the June 1989 flare that was observed in Meudon (Vogt & Hénoux 1999; Emslie et al. 2000).

4. Conclusion

In this paper, we have computed the Hα polarization degree expected when the solar chromosphere is bombarded by a vertically directed beam of non-thermal protons with a power law energy distribution of spectral index 4 or 5. All the processes leading to the population and alignment exchange between sublevels have been taken into account, including charge exchange and the self-consistent effect of the polarization of the local radiation field. While this last effect proved to have only a small effect on the resulting polarization, we found that the polarization is greatly enhanced when using the softer proton spectrum of index 5 compared to the spectral index 4 that was used in previous papers. When the chromosphere is not too hot, a polarization degree of 4–5% can be expected, which is now in better agreement with observed values. When the chromosphere is hot, such as during the maximum phases of a big flare, the polarization is expected to drop to values around or below 1%.

The observed Hα polarization values of 3–6% observed by Vogt et al. (1999) allows us to estimate that the chromosphere was submitted during that flare to a bombardment by a proton beam of spectral index of 5 or greater with a particle flux of a few

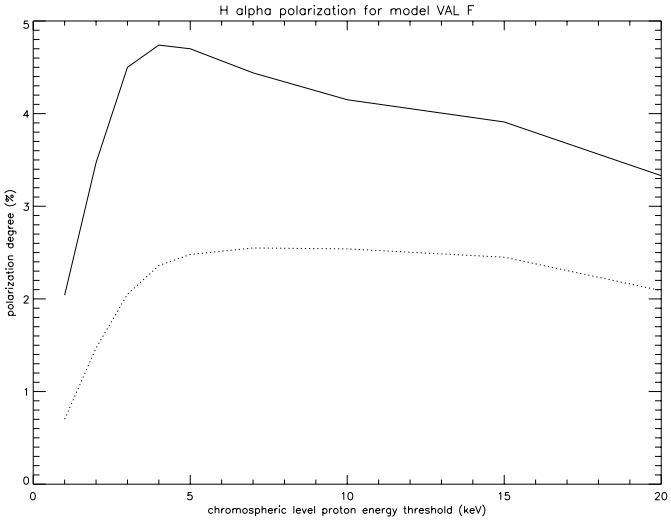

Fig. 3. Hα polarization degree (in percent) as a function of the proton lower energy threshold (in keV) for the initial atmospheric model VAL F, for $\delta = 5$, $\mathcal{F} = 5 \times 10^{16}$ cm^{-2} s^{-1} (plain line) and $\delta = 4$, $\mathcal{F} = 10^{16}$ cm^{-2} s^{-1} (dotted line).

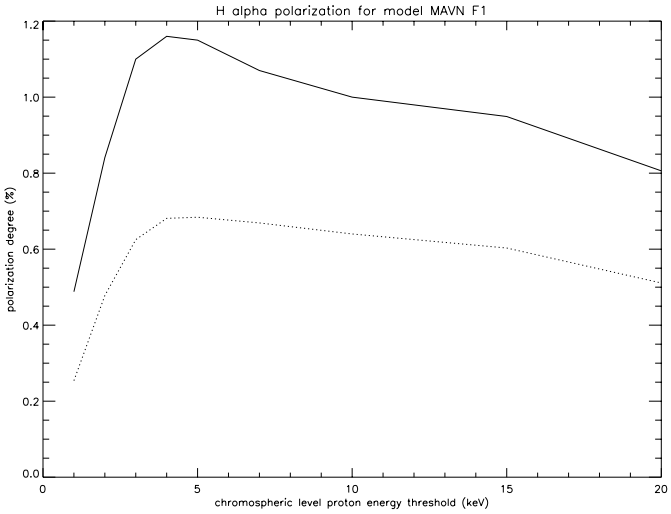

Fig. 4. Hα polarization degree (in percent) as a function of the proton lower energy threshold (in keV) for the initial atmospheric model MAVN F1, for $\delta = 5$, $\mathcal{F} = 5 \times 10^{18}$ cm^{-2} s^{-1} (plain line) and $\delta = 4$, $\mathcal{F} = 5 \times 10^{18}$ cm^{-2} s^{-1} (dotted line).

10^{16} cm^{-2} s^{-1}. A more precise diagnostic would require more information than just the profile integrated polarization degree of the Hα line, such as simultaneous observations in other impact polarization-sensitive lines or the polarization along the line profile. Both information can be obtained with the solar telescope THEMIS in Tenerife (Spain) that is able to observe polarization across the line profiles in several lines simultaneously. Observations made with THEMIS in summer 2000 in the Hα, Hβ and sodium D_1 and D_2 lines are currently being processed (Hénoux & Vogt 2001). The interpretation of THEMIS data will produce a need for further developments to the model of impact polarization presented here such that it can be used for lines other than Hα and can predict the polarization across the line profile (which requires including polarized radiative transfer through the solar atmosphere).

Acknowledgements. Part of this work was done in the frame of the European Solar Magnetometry Network (ESMN) which is funded by the European Commission through a TMR grant.

References

Balança, C. 1997, Ph.D. Thesis, Université Paris XI
Balança, C., & Feautrier, N. 1998, A&A, 334, 1136
Balança, C., & Vogt, E. 1999, in The ninth European meeting on solar physics: magnetic fields and solar processes, ed. A. Wilson, ESA SP-448, 749
Balança, C., & Vogt, E. 2001, in preparation
Bommier, V. 1997, A&A, 328, 706
Emslie, A., Miller, J., Vogt, E., Hénoux, J.-C., & Sahal-Bréchot, S. 2000, ApJ, 542, 513
Fang, C., Hénoux, J.-C., & Gan, W. 1993, A&A, 274, 917
Feautrier, N. 1999, private communication
Hénoux, J.-C., Chambe, G., Smith, D., et al. 1990, ApJS, 73, 303
Hénoux, J.-C., & Vogt, E. 2001, in preparation
Machado, M., Avrett, E., Vernazza, J., & Noyes, R. 1980, ApJ, 242, 336
Landi Degl'Innocenti, E. 1984, Solar Physics, 91, 1
Metcalf, T., Mickey, D., Canfield, R., & Wulser, J.-P. 1994, in High Energy Solar Phenomena, AIP Conf Proc., 294, 59
Metcalf, T., Wulser, J.-P., Canfield, R., & Hudson, H. 1992, in The Compton Observatory Science Workshop, NASA Conf Proc., 3137, 536
Sahal-Bréchot, S., Vogt, E., Thoraval, S., & Diedhiou, I. 1996, A&A, 309, 317
Vernazza, J., Avrett, E., & Loeser, R. 1981, ApJS, 45, 635
Vogt, E. 1997, Ph.D. Thesis, Université Paris VII
Vogt, E., & Hénoux, J.-C. 1996, Solar Physics, 164, 345
Vogt, E., & Hénoux, J.-C. 1999, A&A, 349, 283
Vogt, E., Hénoux, J.-C., & Sahal-Bréchot, S. 1999, in Solar Polarization, ed. K. Nagendra, & J. Stenflo (Kluwer Academic Publishers), ASSL, 243, 431
Vogt, E., Sahal-Bréchot, S., & Hénoux, J.-C. 1997, A&A, 324, 1211, Paper I